

described in Table IV. The catalyst was removed by filtration and was washed with 5 mL of dioxane. The filtrates were combined and evaporated under reduced pressure to leave a pale yellow liquid. The crude product was distilled to afford pure *N*-(2-hydroxyethyl)-3-methyloctylamine: bp 99–101 °C (0.1 mm).

Anal. Calcd for  $C_{11}H_{25}NO$ : C, 72.36; H, 12.56; N, 7.04. Found: C, 72.23; H, 12.60; N, 7.19. (Unsaturated carbon resonances were not present in its  $^{13}C$  NMR spectrum; IR 3400, 3325, 1565  $cm^{-1}$ .) Nitrosation of the secondary amine yielded 2',3',6',6',7',7'-hexahydro-4 (Table IV).

## D-Idose: A One- and Two-Dimensional NMR Investigation of Solution Composition and Conformation

Joseph R. Snyder and Anthony S. Serianni\*

Department of Chemistry, University of Notre Dame, Notre Dame, Indiana 46556

Received November 29, 1985

The solution composition of D-idose in  $D_2O$  has been examined by  $^{13}C$  NMR spectroscopy using  $^{13}C$ -enriched compounds. In addition to two furanoses and two pyranoses, aldehyde and hydrate forms have been detected and quantified. Using  $^{13}C$  saturation-transfer spectroscopy, unidirectional rate constants for ring-opening and -closing of idofuranoses and idopyranoses have been measured and compared. The 600-MHz  $^1H$  NMR spectrum of D-idose has been interpreted, and the  $^{13}C$  spectrum was assigned with the use of 2D  $^{13}C$ - $^1H$  shift correlation spectroscopy.  $^{13}C$  chemical shift assignments were confirmed with  $^{13}C$ -enriched compounds.  $^1H$ - $^1H$  spin-spin couplings suggest the presence of skew forms of  $\alpha$ -idopyranose.

Aqueous solutions of aldoses and ketoses are complex; that is, they contain interconverting pyranose, furanose, hydrate (*gem*-diol, anhydrol), carbonyl, and/or oligomeric forms.<sup>1,2</sup> This complexity has considerable significance in both the chemical and biochemical conversions of the monosaccharides. The spontaneous interconversion of cyclic forms, known as anomerization, has been the subject of numerous studies,<sup>3-5</sup> and recent NMR<sup>6-8</sup> and calculational<sup>9,10</sup> approaches have permitted a more detailed examination of this important reaction. In addition to anomerization, each form may assume one or more stable conformations depending on its structure, adding to the complexity of the system.

The rare aldose, D-idose, while not having major biological significance, is an interesting subject of study for several reasons. Recent  $^{13}C$  NMR studies of D-[1- $^{13}C$ ]-idose<sup>11</sup> have revealed the presence of furanose, pyranose, hydrate, and carbonyl forms in aqueous solution. In ad-

dition, idopyranose rings are conformationally mobile, especially the  $\alpha$ -pyranose.<sup>12a</sup> New conformational free energy values reported by Eliel and co-workers<sup>12b</sup> have been used recently by Augé and David<sup>12c</sup> to reexamine the preferred conformations of ido- and altropyranoses and their derivatives in solution. This study, as well as others, suggests that  $\alpha$ -D-idopyranose may exist in part in a skew conformation ( $S_3^3$ ), although the existing  $^1H$ - $^1H$  spin-coupling data ( $^3J_{H_1,H_2}$ ,  $^3J_{H_2,H_3}$ ) are inconclusive.

A prerequisite to an NMR investigation of idohexose anomerization is the correct assignment of  $^1H$  and  $^{13}C$  NMR spectra, especially signals of the anomeric protons and carbons. These assignments have not been reported. The idose system is a challenging one with which to evaluate various contemporary NMR methods to interpret complex carbohydrate spectra. In this report, one- and two-dimensional NMR are used in conjunction with  $^{13}C$ -enrichment to achieve the complete assignment of  $^1H$  and  $^{13}C$  NMR spectra; the conformational implications of these observed NMR parameters are discussed, with emphasis on pyranosyl ring dynamics. Rate constants of ring-opening and -closing obtained by saturation-transfer NMR spectroscopy are also reported and discussed for the four cyclic forms of D-idose.

### Experimental Section

**Materials.** D-Xylose, D-glucose, and 5% palladium on barium sulfate (Pd/BaSO<sub>4</sub>) were purchased from Sigma Chemical Company. Potassium [ $^{13}C$ ]cyanide (K $^{13}CN$ , 99 atom %  $^{13}C$ ) and deuterium oxide ( $^2H_2O$ , 99.8 atom %  $^2H$ ) were purchased from Cambridge Isotope Laboratories. Standard iodine solutions (0.10 N) were purchased from Fisher Scientific Company. Anhydrous sodium thiosulfate was purchased from Aldrich Chemical Company.

- (1) Angyal, S. J. *Angew. Chem., Int. Ed. Engl.* 1969, 8, 157.
- (2) Angyal, S. J. *Adv. Carbohydr. Chem. Biochem.* 1984, 42, 15.
- (3) Pigman, W.; Isbell, H. S. *Adv. Carbohydr. Chem. Biochem.* 1968, 23, 11.
- (4) Isbell, H. S.; Pigman, W. *Adv. Carbohydr. Chem. Biochem.* 1969, 24, 13.
- (5) Capon, B.; Walker, R. B. *J. Chem. Soc., Perkins Trans. 2* 1974, 1600.
- (6) Serianni, A. S.; Pierce, J.; Huang, S.-H.; Barker, R. *J. Am. Chem. Soc.* 1982, 104, 4037.
- (7) Pierce, J.; Serianni, A. S.; Barker, R. *J. Am. Chem. Soc.* 1985, 107, 2448.
- (8) Goux, W. *J. Am. Chem. Soc.* 1985, 107, 4320.
- (9) Anderson, L.; Garver, J. C. "Computer Modeling of the Kinetics of Tautomerization (Mutarotation) of Aldoses: Implications For the Mechanism of the Process", In *Carbohydrates in Solution*, Advances in Chemistry Series, 117, Gould, R., Ed.; American Chemical Society: Washington, D.C.; 1973; p 20.
- (10) Wertz, P. W.; Garver, J. C.; Anderson, L. *J. Am. Chem. Soc.* 1981, 103, 3916.
- (11) Results of this study were presented at the 189th National Meeting of the American Chemical Society, Division of Carbohydrate Chemistry, April 28–May 3, 1985, Abst. No. 7.

- (12) (a) Angyal, S. J.; Pickles, V. A. *Aust. J. Chem.* 1972, 25, 1695. (b) Eliel, E. L.; Hargrave, K. D.; Pietrusiewicz, K. M.; Manoharan, M. *J. Am. Chem. Soc.* 1982, 104, 3635. (c) Augé, J.; David, S. *Tetrahedron* 1984, 40, 2101.

**Instrumentation.** High-resolution rapid-scan cross-correlation  $^1\text{H}$  NMR spectroscopy at 600 MHz was performed at the NMR Facility for Biomedical Studies, Department of Chemistry, Carnegie-Mellon University, Pittsburgh, PA, which is partly supported by NIH Grant P41RR00292-19.

One-dimensional high-resolution  $^1\text{H}$  (300 MHz) and  $^1\text{H}$ -decoupled  $^{13}\text{C}$  (75 MHz) NMR spectroscopy was performed on a Nicolet NT-300 FT-NMR spectrometer at the Department of Chemistry, University of Notre Dame.  $^1\text{H}$ -Coupled  $^{13}\text{C}$  NMR spectra were obtained with nuclear Overhauser enhancement (NOE) by gating the  $^1\text{H}$  broadband decoupler off during data acquisition. Selective  $^1\text{H}$ -decoupled  $^{13}\text{C}$  NMR spectra were obtained on  $^{13}\text{C}$ -enriched compounds using low-power (0.3 W) coherent  $^1\text{H}$  irradiation in place of high-power (4–5 W) broadband frequency modulation.

To enhance the resolution of  $^1\text{H}$  and  $^{13}\text{C}$  FT-NMR spectra, a double-exponential apodization function was applied to free-induction decays (FIDs) prior to Fourier transformation; FIDs were zero-filled whenever resolution enhancement was applied to achieve acceptable digital resolution (computer points/Hz) in transformed spectra.<sup>13</sup> For observation of the natural abundance portion of  $^{13}\text{C}$ -enriched compounds, spectra were recorded by using block-averaging techniques to minimize dynamic range problems.<sup>13,14</sup>

Two-dimensional  $^{13}\text{C}$ - $^1\text{H}$  chemical shift correlated spectra<sup>15,16</sup> were obtained on the Nicolet NT-300 using software supplied by GE NMR systems.

$^{13}\text{C}$  saturation-transfer NMR spectra were recorded at 75 MHz on the Nicolet NT-300. Spectrometer hardware was modified to permit the application of specific low-power radio frequency (rf) irradiation by the rf transmitter. A pulse program was written to permit transmitter offset, transmitter power, and saturation times to be changed automatically during the experiment. Details of the hardware modification and pulse program are described in the Appendix.

Partially relaxed  $^1\text{H}$  NMR spectra were obtained by inversion-recovery.<sup>17</sup>

**Preparations.** D-Idose was prepared by the addition of KCN (3 molar equiv) to D-xylose (1 molar equiv), followed by catalytic reduction of the product D-idono- and gulononitriles with 5% Pd/BaSO<sub>4</sub> and H<sub>2</sub>, according to published procedures.<sup>18,19</sup> The resulting mixture containing D-idose (15%), D-gulose (75%), and unreacted D-xylose (10%) was purified by column chromatography at room temperature on Dowex 50 × 8 (200–400 mesh) in the calcium form,<sup>20</sup> with distilled water as the eluent. Fractions were assayed for reducing sugar with phenol-sulfuric acid;<sup>21</sup> D-xylose eluted first, D-idose second, followed closely by D-gulose. For large-scale preparations (>25 mmol total hexose), a 15 × 100 cm column was used to achieve separation; for small preparations (<5 mmol total hexose), a 2.5 × 100 cm column was adequate.

D-[1- $^{13}\text{C}$ ]Idose was prepared from D-xylose and K $^{13}\text{C}$ N as described above for the unenriched compound. D-[2- $^{13}\text{C}$ ]Idose was prepared by treating D-[1- $^{13}\text{C}$ ]gulose with molybdc acid<sup>22</sup> and separating the product D-[2- $^{13}\text{C}$ ]idose from D-[1- $^{13}\text{C}$ ]gulose by ion-exchange chromatography<sup>20</sup> (see above). D-[3- $^{13}\text{C}$ ]Idose was prepared by the addition of KCN to D-[2- $^{13}\text{C}$ ]xylose. D-[2- $^{13}\text{C}$ ]-

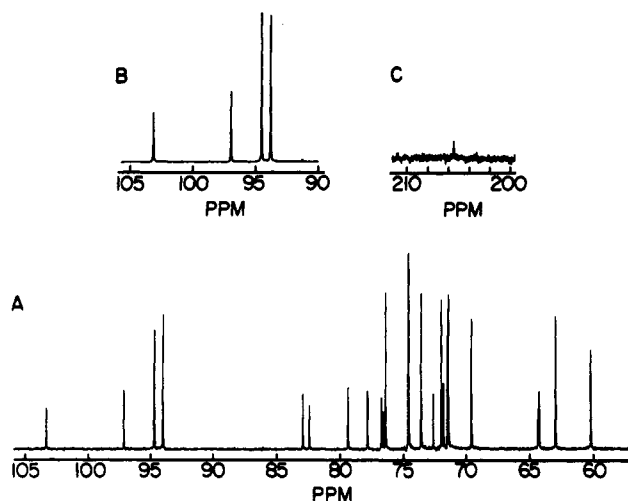
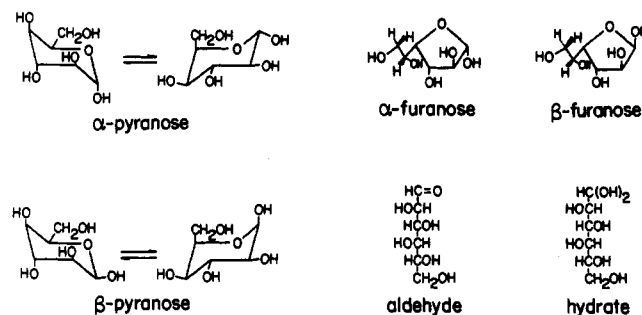


**Figure 1.** (A) The 75-MHz  $^1\text{H}$ -decoupled  $^{13}\text{C}$  NMR spectrum of D-idose in  $^2\text{H}_2\text{O}$ . The four signals between 94 and 104 ppm are the C1 carbons of the four major forms. Signals between 69 and 85 ppm and between 60 and 65 ppm are the C2–C5 and C6 carbons of these forms, respectively. (B) The 90–105-ppm region of the  $^{13}\text{C}$  NMR spectrum of D-[1- $^{13}\text{C}$ ]idose, showing the presence of a small signal at 91.2 ppm attributed to C1 of idose hydrate. (C) The 200–210-ppm region of the  $^{13}\text{C}$  NMR spectrum of D-[1- $^{13}\text{C}$ ]idose, showing a small signal at 205.7 ppm attributed to C1 of idose aldehyde.

#### Scheme I



Xylose was prepared from D-[1- $^{13}\text{C}$ ]lyxose by the action of molybdc acid;<sup>22</sup> labeled xylose and lyxose were separated by ion-exchange chromatography<sup>20</sup> described above (xylose eluted first, followed by lyxose).

D-Glycero-D-[1- $^{13}\text{C}$ ]idoheptose was prepared by the addition of K $^{13}\text{C}$ N to D-glucose, followed by reduction of the labeled heptonitriles.<sup>18,19</sup> A 7-fold molar excess of K $^{13}\text{C}$ N was used in the cyanide addition reaction to promote conversion to nitriles. Separation of unreacted D-glucose (~30%) and the  $^{13}\text{C}$ -labeled heptoses (~70%) was achieved by ion-exchange chromatography<sup>20</sup> (see above); glucose eluted first, idoheptose second, followed closely by guloheptose. Aldose concentrations were determined by quantitative oxidation to aldones with sodium hypiodite.<sup>23</sup>

## Results and Discussion

**1. Identification of Forms of D-Idose in Aqueous Solution.** Angyal and Pickles<sup>12</sup> have shown that aqueous solutions of D-idose contain four major forms, namely,  $\alpha$ -pyranose,  $\beta$ -pyranose,  $\alpha$ -furanose, and  $\beta$ -furanose (Scheme I). Earlier, Angyal<sup>1</sup> calculated interaction energies for idopyranose rings in chair conformations and found free energy differences ( $^4\text{C}_1$ - $^1\text{C}_4$ ) of 0.50 and -1.30 kcal/mol for  $\alpha$ - and  $\beta$ -pyranose, respectively. He concluded that  $\alpha$ -idopyranose exists predominately in the  $^1\text{C}_4$  conformation (70%) while  $\beta$ -idopyranose exists predominately in the  $^4\text{C}_1$  conformation (90%).<sup>1</sup> These conformational assignments were confirmed by measurement of

(13) For a review of digitisation and data processing in Fourier transform NMR, see: Lindon, J. C.; Ferrige, A. G. *Prog. NMR Spectrosc.* 1980, 14, 27.

(14) Davies, S.; Bauer, C.; Barker, P.; Freeman, R. *J. Magn. Reson.* 1985, 64, 155.

(15) Morris, G. A.; Hall, L. D. *J. Am. Chem. Soc.* 1981, 103, 4703.

(16) For a review of 2D NMR spectroscopy of carbohydrates and related compounds, see: *J. Carbohydr. Chem.* 1984, 3.

(17) Vold, R. L.; Waugh, J. S.; Klein, M. P.; Phelps, D. E. *J. Chem. Phys.* 1968, 48, 3831.

(18) Serianni, A. S.; Nunez, H. A.; Barker, R. *Carbohydr. Res.* 1979, 72, 71.

(19) Serianni, A. S.; Barker, R. "Synthetic Approaches to Carbohydrates Enriched With Stable Isotopes of Carbon, Hydrogen and Oxygen", in *Isotopes in the Physical and Biomedical Sciences*, Jones, J., Buncel, E., Eds.; 1986, in press.

(20) Angyal, S. J.; Bethell, G. S.; Beveridge, R. *Carbohydr. Res.* 1979, 73, 9.

(21) Hodge, J. E.; Hofreiter, B. T. *Methods Carbohydr. Chem.* 1962, 1, 380.

(22) Hayes, M. L.; Pennings, N. J.; Serianni, A. S.; Barker, R. *J. Am. Chem. Soc.* 1982, 104, 6764.

(23) Schaffer, R.; Isbell, H. S. *Methods Carbohydr. Chem.* 1963, 2, 11.

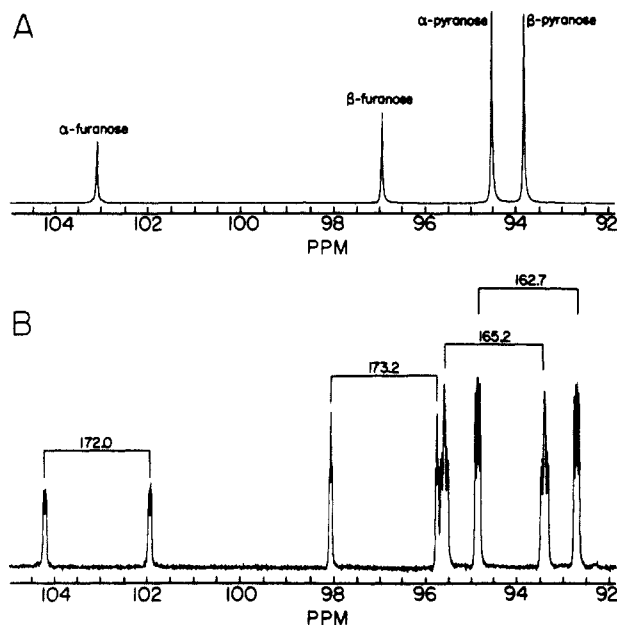


**Figure 2.** (A) The anomeric carbon region of the 75-MHz  $^1\text{H}$ -decoupled  $^{13}\text{C}$  NMR spectrum of D-[1- $^{13}\text{C}$ ]idose, showing signal assignments. (B) The same region as in A of the  $^1\text{H}$ -coupled (with NOE)  $^{13}\text{C}$  NMR spectrum, processed with resolution enhancement. The one-bond  $J_{\text{C,H}}$  coupling for each form is as indicated; longer range ( $^2J_{\text{C,H}}$  and  $^3J_{\text{C,H}}$ ) couplings can also be observed for each form.

$^3J_{\text{H}_1\text{H}_2}$  ( $\alpha$ -pyranose, 6.0 Hz;  $\beta$ -pyranose, 1.6 Hz).<sup>12</sup>

In a recent  $^{13}\text{C}$  NMR study of D-idose,<sup>24a</sup> anomeric carbon resonances were assigned (Figure 1A, 1B) by comparing integrations obtained from  $^1\text{H}$  and  $^{13}\text{C}$  NMR spectra. This approach is subject to considerable error since the pyranoses are present in very similar amounts. A more reliable approach is based on assessment of  $^{13}\text{C}$ - $^1\text{H}$  couplings and selective  $^1\text{H}$ -decoupled  $^{13}\text{C}$  NMR spectra.

**Anomeric Carbon Assignment Based on  $^1J_{\text{C}_1\text{H}_1}$ .** The magnitude of  $^1J_{\text{C}_1\text{H}_1}$  in pyranosyl rings depends on the orientation of the C-H bond, with  $^1J_{\text{C,H}}$  = 160 and 170 Hz for axial and equatorial bonds, respectively.<sup>25</sup> Differences between  $^1J_{\text{C}_1\text{H}_1}$  in furanose anomers are much smaller (1–2 Hz) because the C-H bond in these structures is pseudo-equatorial in both configurations (i.e., C1–O1 bonds in furanosyl rings prefer a quasi-axial orientation due to the anomeric effect).<sup>26,27</sup> However, aldofuranose anomeric carbons can be assigned reliably since their chemical shifts depend strongly on the relative orientations of O1 and O2; C1 signals of anomers with O1–O2 cis are found upfield from those of the corresponding trans anomers.<sup>27,28</sup> It is reasonable, therefore, to assign C1 resonances at 103.1 and 96.8 ppm (Figure 1A, 1B) to  $\alpha$ - and  $\beta$ -idofuranose, respectively.

The  $^1\text{H}$ -decoupled and  $^1\text{H}$ -coupled  $^{13}\text{C}$  NMR spectra of D-[1- $^{13}\text{C}$ ]idose are shown in Figure 2A and 2B. For the pyranose C1 resonances,  $^1J_{\text{C}_1\text{H}_1}$  values of 165.2 and 162.7 Hz are observed for the downfield and upfield pyranose

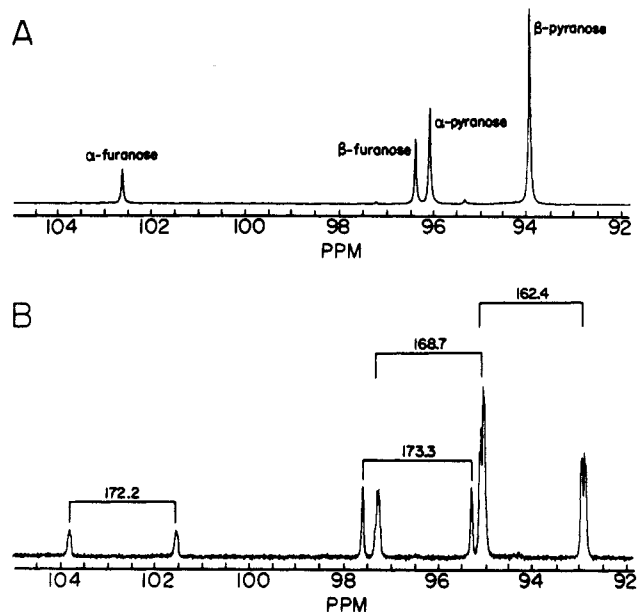


**Figure 3.** (A) The anomeric carbon region of the 75-MHz  $^1\text{H}$ -decoupled  $^{13}\text{C}$  NMR spectrum of D-glycero-D-[1- $^{13}\text{C}$ ]idoheptose, showing signal assignments. (B) The same region as in A of the  $^1\text{H}$ -coupled (with NOE)  $^{13}\text{C}$  NMR spectrum, processed with resolution enhancement. The one-bond  $J_{\text{C,H}}$  coupling for each form is as indicated; longer range ( $^2J_{\text{C,H}}$  and  $^3J_{\text{C,H}}$ ) couplings can also be observed for each form.

signals, respectively. From the chair distribution discussed above,  $^1J_{\text{C}_1\text{H}_1}$  for the  $\alpha$ -pyranose is predicted to be larger than that for the  $\beta$ -pyranose, suggesting that the downfield signal be assigned to the  $\alpha$ -pyranose. This assignment, however, is inconsistent with that made recently by Grindley and Gulasekhar.<sup>24a</sup>

The  $^1\text{H}$ -coupled  $^{13}\text{C}$  NMR spectra of D-glycero-D-[1- $^{13}\text{C}$ ]idoheptose was examined to check the validity of this approach. Idoheptopyranosyl rings are similar configurationally to idopyranosyl rings, making this comparison ideal. Angyal and Tran<sup>29</sup> have shown that both  $\alpha$ - and  $\beta$ -D-glycero-D-idoheptoses exist predominantly in the  $^4\text{C}_1$  conformation and have assigned the anomeric carbon signals. As shown in Figure 3A and 3B,  $^1J_{\text{C}_1\text{H}_1}$  values of 168.7 and 162.4 Hz found for  $\alpha$ - and  $\beta$ -idoheptopyranoses, respectively, are consistent with their preferred chair forms and demonstrate that the idopyranose ring does not depart from the general relationship between  $^1J_{\text{C}_1\text{H}_1}$  and pyranose anomeric configuration.

**Anomeric Carbon Assignment Based on Double-Resonance Methods.** Anomeric carbon assignments were verified by selectively saturating the anomeric protons while observing the  $^{13}\text{C}$  NMR spectrum of D-[1- $^{13}\text{C}$ ]idose. The anomeric proton resonances (5.20 ppm,  $\alpha$ -furanose; 5.41 ppm,  $\beta$ -furanose; 4.97 ppm,  $\alpha$ -pyranose; 5.05 ppm,  $\beta$ -pyranose)<sup>12</sup> are resolved sufficiently at 300 MHz to permit selective saturation. As shown in Figure 4B,  $^1\text{H}$  irradiation at 5.41 ppm collapsed the  $^{13}\text{C}$  signal at 96.8 ppm, indicating that these two nuclei are bonded together. Separate  $^1\text{H}$  irradiation at 5.20, 5.05, and 4.97 ppm collapsed carbon signals at 103.1, 93.7, and 94.4 ppm, respectively (Figure 4C–E).

The two-dimensional  $^{13}\text{C}$ - $^1\text{H}$  shift correlation spectrum of the anomeric region (Figure 4F) is consistent with conclusions drawn from  $^1J_{\text{C}_1\text{H}_1}$  analysis and selective  $^1\text{H}$ -decoupled  $^{13}\text{C}$  NMR spectra. Therefore, the correct assignment of anomeric carbons of D-idose is  $\alpha$ -furanose,

(24) (a) Grindley, T. B.; Gulasekhar, V. *J. Chem. Soc., Chem. Commun.* 1978, 1073. (b) During the preparation of this manuscript, a report (Reuben, J. *J. Am. Chem. Soc.* 1985, 107, 5867) appeared in which deuterium isotope shift effects were used to assign the  $^{13}\text{C}$  NMR spectrum of D-idose. Our assignments differ from these for the closely spaced C2 and C3 signals of  $\beta$ -idopyranose. Using [2- $^{13}\text{C}$ ] and [3- $^{13}\text{C}$ ]idose, we have confirmed that, under our experimental conditions, C3 is upfield of C2.

(25) Bock, K.; Pedersen, C. *Acta Chem. Scand., Ser. B* 1977, B31, 354.

(26) Cyr, N.; Perlin, A. S. *Can. J. Chem.* 1979, 57, 2504.

(27) Serianni, A. S.; Barker, R. *J. Org. Chem.* 1984, 49, 3292.

(28) Ritchie, R. G. S.; Cyr, N.; Korsch, B.; Koch, H. J.; Perlin, A. S. *Can. J. Chem.* 1975, 53, 1424.

(29) Angyal, S. J.; Tran, T. Q. *Aust. J. Chem.* 1983, 36, 937.

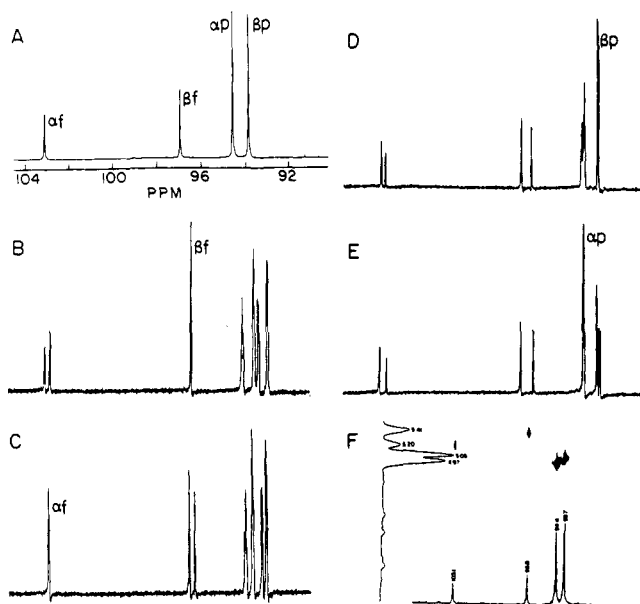


**Figure 4.** (A) The 75-MHz  $^{13}\text{C}$  NMR spectrum of D-[1- $^{13}\text{C}$ ]idose (anomeric carbon region). (B-E) Selective  $^1\text{H}$ -decoupled  $^{13}\text{C}$  NMR spectra of the anomeric carbons of D-[1- $^{13}\text{C}$ ]idose, showing the effect of specific  $^1\text{H}$  irradiation at 5.41 ppm (B), 5.20 ppm (C), 5.05 ppm (D), and 4.97 ppm (E) on carbon signal multiplicity, allowing the assignment of carbon signals to specific forms. (F) The 2D  $^{13}\text{C}$ - $^1\text{H}$  shift correlation contour map of the anomeric  $^{13}\text{C}$  and  $^1\text{H}$  regions of D-idose, confirming the signal assignments based on  $^1\text{H}$ -coupled  $^{13}\text{C}$  NMR spectra (B-E).

103.1 ppm;  $\beta$ -furanose, 96.8 ppm;  $\alpha$ -pyranose, 94.4 ppm;  $\beta$ -pyranose, 93.7 ppm.

In addition to cyclic forms, D-idose can exist in two linear forms, namely, aldehyde and hydrate (*gem*-diol, anhydrol) (Scheme I). In general, these forms are present in minor amounts in aqueous solutions of aldohexoses, but their proportions increase substantially as the length of the carbon chain decreases. For example, D-glucose aldehyde is believed to comprise about 0.003 mol % of glucose solutions,<sup>30</sup> whereas the aldehyde represents  $\sim 2$  mol % in D-erythrose solutions.<sup>6,7,31</sup> Detection of these minor forms is greatly facilitated by selective [ $^{13}\text{C}$ ]-enrichment at the anomeric carbon. The  $^{13}\text{C}$  NMR spectrum of D-[1- $^{13}\text{C}$ ]idose (Figure 1B, 1C) reveals small resonances at 91.2 and 205.7 ppm attributed to idose hydrate and aldehyde, respectively. C1,H1 couplings for these resonances are 162.6 and  $\sim 182$  Hz, respectively, values observed previously for similar linear forms.<sup>27,32,33</sup>

To further demonstrate that the signal at 205.7 ppm is indeed aldehyde and not a minor contaminant, a saturation-transfer experiment<sup>34,35</sup> was conducted wherein the presumed aldehyde C1 resonance was saturated for varying times and the effect of this saturation on the intensities of the C1 resonances of the cyclic forms monitored. If the saturated carbon is chemically exchanging with the remaining C1 carbons, this exchange will be indicated by a time-dependent loss in intensity of these carbon signals. Transfer of saturation is observed (Figure 5).

As described in detail previously,<sup>6,7</sup> saturation-transfer can be used to obtain ring-opening rate constants of

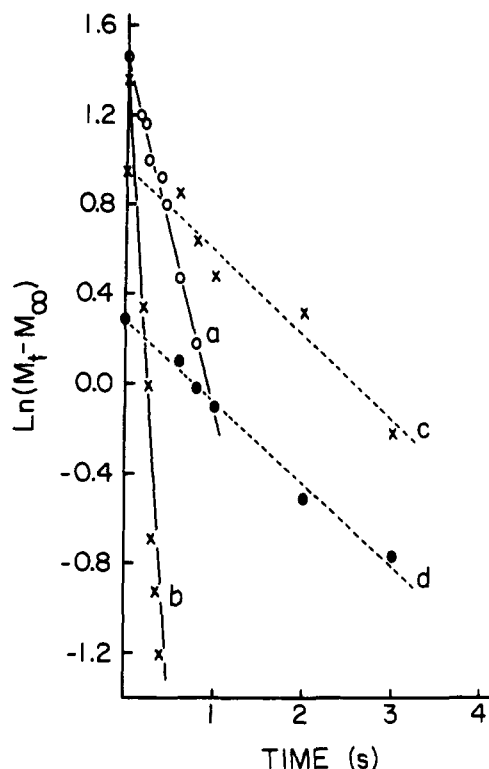


**Figure 5.** The effect of saturation of C1 idose aldehyde on the C1 resonance intensities of the cyclic forms of D-[1- $^{13}\text{C}$ ]idose: (a)  $\alpha$ -furanose, (b)  $\beta$ -furanose, (c)  $\alpha$ -pyranose, (d)  $\beta$ -pyranose. Solution conditions: 0.25 M aldose, 50 mM KCl, and pH 2.0 (HCl), 40  $^\circ\text{C}$ . From these data, ring-opening rate constants were determined:  $1.3\text{ s}^{-1}$  ( $\alpha$ -furanose),  $6.3\text{ s}^{-1}$  ( $\beta$ -furanose),  $0.04\text{ s}^{-1}$  ( $\alpha$ -pyranose), and  $0.06\text{ s}^{-1}$  ( $\beta$ -pyranose).

anomerization in solution. These rate constants will be discussed below.

Examination of the  $^{13}\text{C}$  NMR spectrum of D-glycero-D-[1- $^{13}\text{C}$ ]idoheptose also reveals small signals at 205.8 ppm (aldehyde,  $^1J_{\text{C1,H1}} = 182.4$  Hz) and 91.3 (hydrate,  $^1J_{\text{C1,H1}} = 163.9$  Hz) in addition to major signals at 102.6 ( $\alpha$ -furanose), 96.4 ( $\beta$ -furanose), 96.1 ( $\alpha$ -pyranose), and 94.0 ppm ( $\beta$ -pyranose).

**2. Proportion of Forms of D-Idose and D-Glycero-D-idoheptose in Aqueous Solution.** The proportion of forms of a reducing sugar in solution depends on the solvent and temperature. From the  $^{13}\text{C}$  NMR spectrum of the [ $^{13}\text{C}$ ]-enriched compound obtained at 30  $^\circ\text{C}$  in water (approximately 0.7 M aldose), D-idose exists as follows:  $\alpha$ -furanose, 13.5%;  $\beta$ -furanose, 16.5%;  $\alpha$ -pyranose 35.9%;  $\beta$ -pyranose, 33.4%; hydrate, 0.5%; aldehyde, 0.1%. The same percentages are calculated from the  $^1\text{H}$ -decoupled  $^{13}\text{C}$  NMR spectrum obtained without NOE.

Under the same conditions, D-glycero-D-idoheptose exists as follows:  $\alpha$ -furanose, 8.7%;  $\beta$ -furanose, 15.5%;  $\alpha$ -pyranose, 24.4%;  $\beta$ -pyranose, 50.8%; hydrate, 0.6%; aldehyde, 0.06%.

It is interesting to note that the trans O1-O2 idofuranose and idoheptofuranose anomers are less stable thermodynamically than the corresponding cis anomers. Aldofuranoses having the xylo configuration generally exhibit this characteristic, in contrast to furanoses having ribo, arabino, and lyxo configurations. Apparently, the instability caused by two 1,3-interactions (O1-C5 and O1-O3) in the O1-O2 trans anomer is greater than that imposed by an unfavorable O1-O2 interaction in the corresponding cis anomer. As discussed below, despite its greater thermodynamic stability, the O1-O2 cis anomer opens faster to the linear aldehyde.

(30) Los, J. M.; Simpson, L. B.; Wiesner, K. *J. Am. Chem. Soc.* **1956**, *78*, 1564.

(31) Angyal, S. J.; Wheen, R. G. *Aust. J. Chem.* **1980**, *33*, 1001.

(32) Serianni, A. S.; Pierce, J.; Barker, R. *Biochemistry* **1979**, *18*, 1192.

(33) Serianni, A. S.; Clark, E. L.; Barker, R. *Carbohydr. Res.* **1979**, *72*, 79.

(34) Forsén, S.; Hoffman, R. A. *J. Chem. Phys.* **1963**, *39*, 2892.

(35) Mann, B. E. *J. Magn. Reson.* **1976**, *21*, 17.

Table I.  $^1\text{H}$  and  $^{13}\text{C}$  NMR Chemical Shift Assignments<sup>a</sup> for D-Idose in  $^2\text{H}_2\text{O}$ 

compd	chemical shift (ppm)												
	H1	H2	H3	H4	H5	H6	H6'	C1	C2	C3	C4	C5	C6
$\alpha$ -furanose	5.19	4.10				3.72	3.61	103.1	82.4	76.5	82.9	72.6	64.3
$\beta$ -furanose	5.41		4.29		3.88	3.66	3.58	96.8	77.8	76.7	79.3	71.7	64.2
$\alpha$ -pyranose	4.97	3.39	3.67	3.79	4.15	3.83	3.75	94.4	74.5	73.5	71.9	74.5	60.1
$\beta$ -pyranose	5.05	3.67	4.05	3.64	3.99	3.81	3.77	93.7	71.4	71.3	69.5	76.3	62.9

<sup>a</sup> Values reported in ppm.  $^1\text{H}$  values are relative to internal sodium 3-(trimethylsilyl)-1-propanesulfonate and are accurate to  $\pm 0.01$  ppm.  $^{13}\text{C}$  values are referenced (external) to the anomeric carbon of  $\beta$ -D-[1- $^{13}\text{C}$ ]glucopyranose (97.4 ppm) and are accurate to  $\pm 0.1$  ppm.

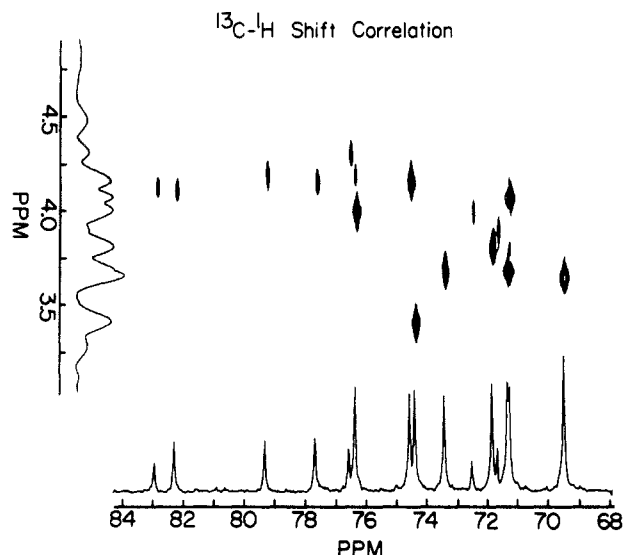


Figure 6.  $^{13}\text{C}$ - $^1\text{H}$  chemical shift correlation contour map of D-idose (C2-C5 region). The spectra displayed along each axis were obtained by  $0^\circ$  and  $90^\circ$  projections of the data. The projected  $^1\text{H}$  spectrum is of low resolution, but nevertheless sufficient to extract useful bonding correlations.

Table II.  $^1\text{H}$ - $^1\text{H}$  Spin-Coupling Constants<sup>a</sup> for D-Idose in  $^2\text{H}_2\text{O}$ 

compd	$J_{\text{HH}}$ (Hz)							
	1,2	2,3	3,4	4,5	5,6	5,6'	6,6'	2,4
$\alpha$ -furanose	1.3	2.2			4.0	6.6	-11.8	
$\beta$ -furanose	4.3	5.4	5.0	5.0	4.4	7.1	-11.7	
$\alpha$ -pyranose	6.0	8.1	7.9	5.0	8.8	3.9	-12.4	
$\beta$ -pyranose	1.6	3.8	3.7	1.8	7.5	4.4	-11.8	1.2

<sup>a</sup> Values are reported in hertz and are accurate to  $\pm 0.1$  Hz. Measured at  $\sim 25^\circ\text{C}$ .

**3. Assignment of  $^1\text{H}$  and  $^{13}\text{C}$  NMR Spectra of D-Idose (Nonanomeric Regions).** The  $^{13}\text{C}$  NMR spectrum of D-idose (Figure 1A) contains 24 well-resolved signals, 6 signals from each cyclic form. Assignment of the anomeric carbon resonances was described above. A 2D  $^{13}\text{C}$ - $^1\text{H}$  chemical shift correlation spectrum was obtained (Figure 6) to assign the remaining spectrum. From this map, multiplets in the 300-MHz  $^1\text{H}$  NMR spectrum could be correlated with  $^{13}\text{C}$  signals (Figure 7A). However, the complexity of the resolution-enhanced 300-MHz  $^1\text{H}$  NMR spectrum still prevents assignment of most protons to individual forms. Obtaining a partially relaxed  $^1\text{H}$  NMR spectrum does separate some multiplets due to differences in relaxation rates between protons (Figure 7B). For example, hydroxymethyl protons generally relax faster than methine protons due to the proximity of the methylene protons to each other. This allows the methylene proton resonances to be resolved from the more slowly relaxing methine protons. Examination of the 3.8-ppm region (Figure 7B) clearly shows the presence of a more slowly relaxing quartet amidst more rapidly relaxing hydroxymethyl protons.

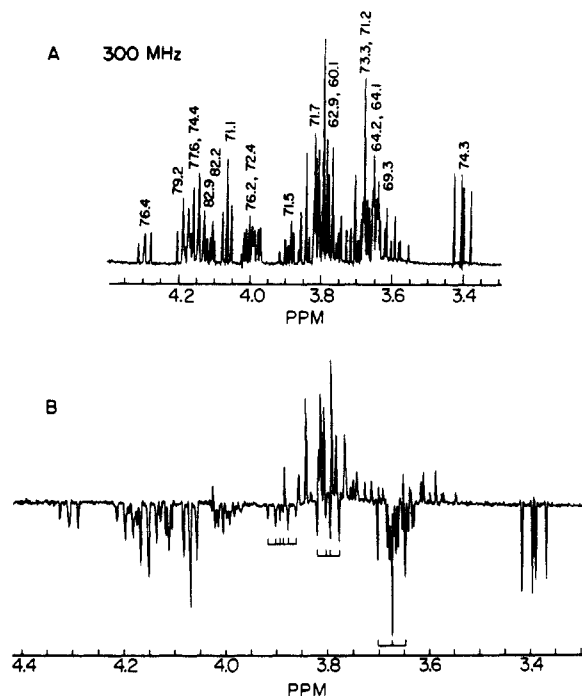


Figure 7. (A) The 300-MHz  $^1\text{H}$  NMR spectrum of D-idose (nonanomeric region), showing the correlation between specific proton multiplets and individual carbon signals (Figure 1). These correlations were determined from data in Figure 6. (B) A partially relaxed 300-MHz  $^1\text{H}$  NMR spectrum of D-idose (nonanomeric region) showing the different proton relaxation rates in the sample. This differential relaxation helps to simplify complex spectra by separating overlapping multiplets as shown by the brackets.

Table III.  $^{13}\text{C}$  NMR Parameters<sup>a</sup> for 5-O-Methyl-D-xylose<sup>b</sup>

compd	$\delta_{\text{C1}}$	$\delta_{\text{C2}}$	$\delta_{\text{C3}}$	$\delta_{\text{C4}}$	$\delta_{\text{C5}}$	$\delta_{\text{CH}_3}$	$^1J_{\text{C1,C2}}$
$\alpha$ -furanose	95.8	76.4	75.4	76.9	71.2	58.7	42.5
$\beta$ -furanose	102.1	80.8	75.3	76.9	71.8	58.7	45.5

<sup>a</sup> Chemical shifts ( $\delta$ ) are reported in ppm, are referenced (external) to the anomeric carbon of  $\beta$ -D-[1- $^{13}\text{C}$ ]glucopyranose (97.4 ppm), and are accurate to  $\pm 0.1$  ppm.  $J$  values are reported in hertz and are accurate to  $\pm 0.1$  Hz. <sup>b</sup> Carbon assignments were made from 2D  $^{13}\text{C}$ - $^1\text{H}$  chemical shift correlation.<sup>15</sup>

The 600-MHz rapid-scan cross-correlated  $^1\text{H}$  NMR spectrum of D-idose is shown in Figure 8A. Many of the proton multiplets are well resolved at this field strength and appear essentially first order. For example, the 3.70-3.90-ppm region of the spectrum is shown in expanded form in Figure 8B. As suggested from the partially relaxed spectrum (Figure 7B), this region contains 5-hydroxymethyl protons (H6 and H6' of both pyranoses, and H6 of the  $\alpha$ -furanose), H5  $\beta$ -furanose, and H4  $\alpha$ -pyranose. The H4  $\alpha$ -pyranose quartet (hatched signals) is now recognized as the slowly relaxing quartet observed in the same region of the partially relaxed 300-MHz spectrum (Figure 7B).

Proton chemical shift assignments and  $^1\text{H}$ - $^1\text{H}$  couplings obtained from the 600-MHz spectrum are given in Tables I and II; from these data and the  $^{13}\text{C}$ - $^1\text{H}$  correlation map

Table IV.  $^{13}\text{C}$ - $^1\text{H}$  and  $^{13}\text{C}$ - $^{13}\text{C}$  Coupling Constants<sup>a</sup> for D-Idose

compd	coupled nuclei							
	C1-H1	C1-H2	C2-H1	C1-C2	C1-C3	C1-C4	C1-C5	C1-C6
$\alpha$ -furanose	171.9		br	45.2	2.7	0	1.3	0
$\beta$ -furanose	173.2		3.8	42.3	2.2	0	2.2	0
$\alpha$ -pyranose	165.2	4.7	0	46.2	2.5	0	1.1	1.8
$\beta$ -pyranose	162.8		6.1	43.8	0	0	0	3.1

<sup>a</sup> Values are reported in hertz and are accurate to  $\pm 0.1$  Hz. Br denotes broadening.

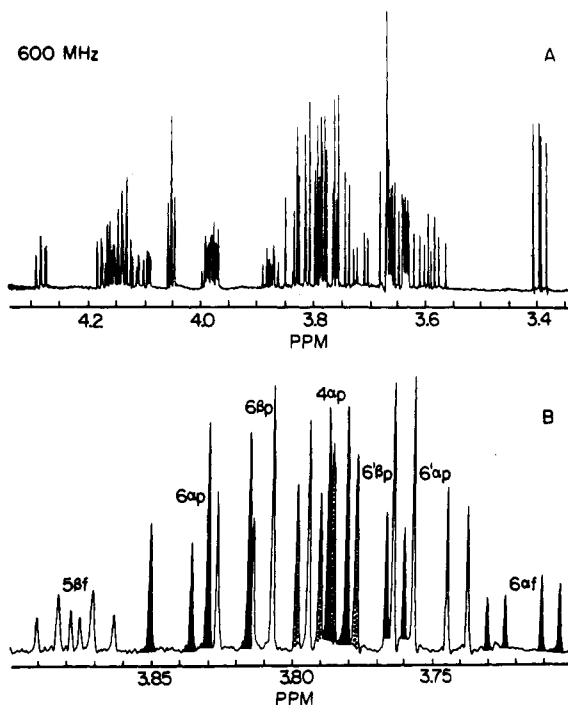


Figure 8. (A) The 600-MHz  $^1\text{H}$  NMR spectrum of D-idose (nonanomeric region), showing the increase in signal dispersion (compared to 300-MHz spectrum, Figure 7A) that facilitated interpretation. (B) An expanded region (3.70–3.90 ppm) of A, showing distinct multiplets for the indicated assigned protons.

(Figure 6),  $^{13}\text{C}$  chemical shift assignments were made (Table I, Figure 9).<sup>24b</sup>

**4. Analysis of  $^1\text{H}$  and  $^{13}\text{C}$  NMR Parameters of D-Idose.** D-Idofuranoses (Scheme I) are related structurally to 5-O-methyl-D-xylose, and comparison of NMR parameters between these compounds is valuable.  $^{13}\text{C}$  chemical shifts of the 5-substituted pentose are given in Table III. The relative positions of  $^{13}\text{C}$  signals for these two compounds are similar, except for the signals of C2 and C4 in the O1–O2 trans anomers. In  $\alpha$ -idofuranose, C2 is upfield from C4, whereas in 5-O-methyl- $\beta$ -xylofuranose the reverse is found. This observation points clearly to the hazards encountered when making assignments based solely on chemical shift comparisons between closely related structures.

As discussed above, relative C1 chemical shifts of aldofuranose anomers depend highly in the orientation of O1–O2 in the structure, with trans orientations giving C1 signals downfield from the corresponding cis orientation. In addition to this useful relationship, a dependence exists between aldofuranose anomeric configuration and  $^1J_{\text{C}_1\text{C}_2}$ , namely, trans O1–O2 configurations yield larger  $^1J_{\text{C}_1\text{C}_2}$  values ( $\sim 45$  Hz) than cis O1–O2 configurations ( $\sim 43$  Hz) (Table IV).

**D-Idopyranoses.** Previous conformational studies of D-idose have been based on analysis of H1 chemical shift and  $^1J_{\text{H}_1\text{H}_2}$ , since only the anomeric protons could be resolved at lower fields. The complete  $^1\text{H}$ – $^1\text{H}$  couplings for the  $\alpha$ -pyranose (Table II) show that, in the chair form, this

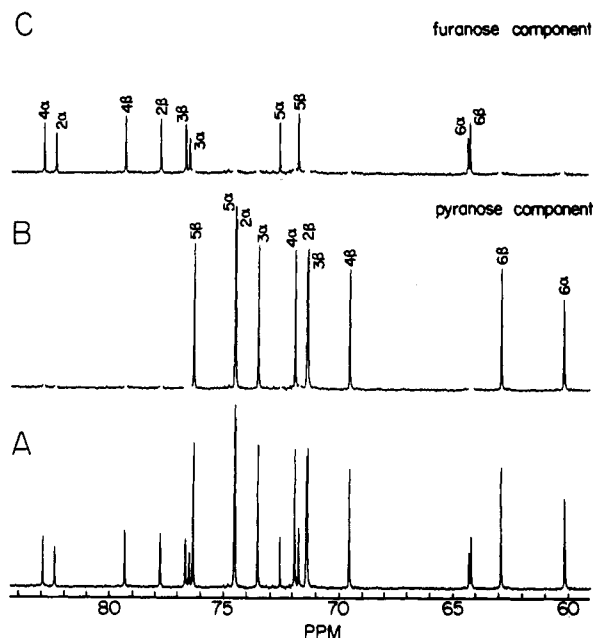


Figure 9. (A) The 60–85-ppm region of the  $^{13}\text{C}$  NMR spectrum of D-idose. (B) The pyranose component edited from the spectrum in A, showing assignments. (C) The furanose component edited from the spectrum in A, showing assignments.

anomer appears to prefer the  $^1\text{C}_4$  conformation. Observed couplings between H1–H2, H2–H3, and H3–H4 more closely correspond to diaxial (for  $^1\text{C}_4$ ) than to diequatorial ( $^4\text{C}_1$ ) orientations. However, the observed coupling between H4–H5 (5.0 Hz) is larger than expected for an axial–equatorial orientation (which exists in both chair forms) and may indicate either deviation from ideal chair behavior and/or deviation from normal “Karplus” behavior in the C4–C5 fragment; by comparison,  $^3J_{\text{H}_4\text{H}_5} = 1.1$  Hz in the conformationally rigid ( $^4\text{C}_1$ ) methyl  $\beta$ -D-galactopyranoside<sup>36a</sup> where these protons are oriented equatorial–axial. If standard values of 9.5 Hz and 2.0 Hz are assumed for diaxial and diequatorial couplings, respectively, for H2–H3 and H3–H4 pairs, then  $^4\text{C}_1/{}^1\text{C}_4 = 0.25$  for  $\alpha$ -D-idopyranose. The larger than expected H4–H5 coupling may indicate that  $\alpha$ -D-idopyranose may exist in a skew conformation,  $S_5^{12c,36b}$ . In this form, the ideal chair-form dihedral angle between H4 and H5 ( $60^\circ$ ) would be reduced, depending on the extent of ring deformation, resulting in a greater coupling between these protons. This deformation would not significantly affect couplings between the other ring protons, which remain anti periplanar (or essentially so) in the  $^1\text{C}_4$  and  $S_5^3$  conformers.

$^1\text{H}$ – $^1\text{H}$  couplings in  $\beta$ -D-idopyranose indicate that this anomer prefers the  $^4\text{C}_1$  conformation; on the basis of H2–H3 and H3–H4 couplings, this pyranose exists 75% as  $^4\text{C}_1$  and 25% as  $^1\text{C}_4$  ( $^4\text{C}_1/{}^1\text{C}_4 = 3.0$ ). Additional evidence for this conformational preference lies in the long-range  $^1\text{H}$ – $^1\text{H}$

(36) (a) Hayes, M. L.; Serianni, A. S.; Barker, R. *Carbohydr. Res.* 1982, 100, 87. (b) Hough, L.; Richardson, A. C. In *Rodd's Chemistry of Carbon Compounds*; Coffey, S., Ed.; 1967; Vol. 1F, Chapter 23.

coupling ( $^4J_{\text{HH}}$ ) observed between H2 and H4 (Table II). Theoretical and experimental studies of four-bond  $^1\text{H}$ - $^1\text{H}$  coupling in saturated systems by Barfield and co-workers<sup>37</sup> have shown that maximal couplings occur in HCCC fragments in which all five atoms lie in the same plane in a W-shaped arrangement. This condition is satisfied in  $\beta$ -D-idopyranose in the  $^4C_1$  conformation.

$^{13}\text{C}$ - $^{13}\text{C}$  coupling between C1 and C6 in pyranoses is also sensitive to chair conformation;<sup>38</sup> dihedral angles of  $60^\circ$  and  $180^\circ$  exist between C1 and C6 in  $^1C_4$  and  $^4C_1$  conformers, respectively.  $^3J_{\text{C}_1, \text{C}_6}$  in  $\alpha$ - and  $\beta$ -D-idopyranoses of 1.8 and 3.1 Hz, respectively, are consistent with their preferred  $^1C_4$  (or  $S_5^3$ ) and  $^4C_1$  conformations. A complete analysis of  $^{13}\text{C}$ - $^{13}\text{C}$  coupling in [ $^{13}\text{C}$ ]-enriched aldoses will be presented elsewhere.<sup>39</sup>

**5. Idose Aldehyde and Anomerization.** The aldehyde form of D-idose can be observed by  $^{13}\text{C}$  NMR using [ $^{13}\text{C}$ ]-enrichment (Figure 1C). This represents the first observation of the carbonyl form of an aldohexose by  $^{13}\text{C}$  NMR spectroscopy. It is generally held that aqueous solutions of the higher aldoses contain very minor amounts of linear forms. Nevertheless, aqueous solutions of other [ $^{13}\text{C}$ ]-enriched aldoses (e.g., D-talose, D-ribose) also contain aldehyde in measurable quantities; for example, we estimate approximately 0.03% aldehyde in aqueous solutions of ribose.<sup>40</sup> Detection of minor species in the presence of major forms by FT methods is hindered by dynamic range problems which can be minimized with block-averaging and the acquisition of double-precision data. ADC (analog-to-digital converter) difficulties can be overcome by hardware modifications described recently by Davies et al.<sup>14</sup> Despite these problems, it appears that  $^{13}\text{C}$  NMR in conjunction with [ $^{13}\text{C}$ ]-enrichment at anomeric sites will provide the means to study carbonyl, hydrate, and other minor forms of sugars in the solution state.

In addition to detection and quantitation, the observation of idose aldehyde permits studies of anomerization in a system that contains significant proportions of furanose and pyranose forms at equilibrium. Ring-opening rate constants for the four anomers can be obtained (Figure 5) by saturation-transfer NMR methods. Previous studies<sup>10</sup> based on kinetic modeling of gas-chromatographic data suggested that ring-opening rates of pyranoses are much slower than those of furanoses. At  $40^\circ\text{C}$  and pH 2.0, ring-opening rate constants were determined in a single experiment and are as follows:  $\alpha$ -furanose,  $1.3\text{ s}^{-1}$ ;  $\beta$ -furanose,  $6.3\text{ s}^{-1}$ ;  $\alpha$ -pyranose,  $0.04\text{ s}^{-1}$ ;  $\beta$ -pyranose,  $0.06\text{ s}^{-1}$ . Under conditions of acid catalysis, idopyranoses open approximately 75 times more slowly than idofuranoses. In addition, rates of ring-opening depend on anomeric configuration, with the *cis* O1-O2 furanose opening approximately 5 times faster than the *trans* compound; this observation is consistent with those made previously on xylo ring systems.<sup>7</sup> While there appears to be a difference in ring-opening rate constants between  $\alpha$ - and  $\beta$ -idopyranoses, this observation remains to be verified under conditions where the exchange rates are more rapid.

From equilibrium constants (e.g., [ $\alpha$ -pyranose]/[aldehyde]) determined at  $40^\circ\text{C}$  at pH 2.0, we estimate ring-closing rate constants in the idose system:  $\alpha$ -furanose,  $6.2 \times 10^2\text{ s}^{-1}$ ;  $\beta$ -furanose,  $3.8 = 10^3\text{ s}^{-1}$ ;  $\alpha$ -pyranose,  $4.6 \times 10^1\text{ s}^{-1}$ ;  $\beta$ -pyranose,  $6.6 \times 10^1\text{ s}^{-1}$ . These values are subject to error due to uncertainties in determining aldehyde con-

centration, but the data indicate that ring-closure for furanoses is significantly faster than for pyranoses. Previous studies<sup>10</sup> on D-galactose anomerization at pH 4.3 and 6.2 indicated that ring-opening rate constants were similar for furanoses and pyranoses, although these authors state clearly that this conclusion is unexpected. Our data suggests that for both ring-opening and ring-closing reactions idofuranoses react faster than idopyranoses. This observation is consistent with the behavior of sugars like D-talose in aqueous solution. Dissolution studies of  $\alpha$ -D-[ $^{13}\text{C}$ ]-talopyranose show a rapid formation of both furanoses *prior* to the generation of significant amounts of  $\beta$ -D-[ $^{13}\text{C}$ ]-talopyranose.<sup>40</sup> In fact, furanose concentrations increase beyond their final equilibrium concentrations early in the reaction, when they are competing with  $\alpha$ -pyranose only. Unfortunately, we cannot fit our experimental rate constants using rate equations describing four-components interconverting through a common intermediate<sup>9</sup> because crystalline forms of D-idose are not available. We are, however, pursuing this approach with D-talose.<sup>40</sup>

One aim of studies of monosaccharide anomerization is to understand the driving force(s) behind ring-opening and -closing and to decipher the mechanism by which these reactions take place. Nucleophilic attack at C1 of idose aldehyde by O4 is more preferred than that by O5, even though pyranoses predominate at equilibrium (because ring-opening is also faster in the furanoses). This enhanced reactivity must be due to the ability of O4 to better orient on an orbital trajectory that leads to productive ring closure more frequently than O5 (entropic contribution). Increased reactivity could also be due to a greater nucleophilicity of O4 (enthalpic contribution). The conformational dynamics of the linear aldehyde must play a role in O4 orientation, but nothing is known of this feature at present.

Possible driving forces for ring-opening are even less obvious. Furanoses open faster than pyranoses, suggesting a relationship between ring stability and ring-opening, but an explanation of kinetics in thermodynamic terms is never justified. For example,  $\beta$ -D-idofuranose is more stable (there is a higher proportion at equilibrium) yet opens more rapidly than  $\alpha$ -D-idofuranose. It is possible that differences in ring protonation and/or protonation-abstractation may account for differences in ring-opening rates.

### Conclusions

Aqueous solutions of many reducing monosaccharides contain substantial quantities of furanose and pyranose forms. Interpretation of  $^1\text{H}$  and  $^{13}\text{C}$  NMR spectra of these compounds can be complicated; four forms of an aldohexose in  $^2\text{H}_2\text{O}$  will generate a maximum of 24  $^{13}\text{C}$  signals and 28  $^1\text{H}$  signals, the latter further split by homonuclear coupling. This study has shown that, in these systems, the use of [ $^{13}\text{C}$ ]-enrichment, 2D  $^{13}\text{C}$ - $^1\text{H}$  shift correlation spectroscopy, very high field  $^1\text{H}$  NMR spectroscopy, and several double-resonance one-dimensional NMR methods permit a complete analysis of their spectra.

Use of two-dimensional shift-correlated spectra clearly facilitated the present study. In contrast, COSY and SECSY experiments, which were conducted at 300 MHz (data not reported), were complex and did not yield information not obtainable from the 300-MHz 1D  $^1\text{H}$  NMR spectrum. Despite the availability of 2D methods, therefore, the need to obtain very high field (600 MHz) 1D  $^1\text{H}$  NMR spectra was real.

Results of this investigation are summarized as follows: (a) The anomeric carbon signals for  $\alpha$ - and  $\beta$ -D-idopyranoses have been reassigned. (b)  $^1\text{H}$  (600 MHz) and  $^{13}\text{C}$  (75 MHz) NMR spectra of D-idose have been obtained

(37) Barfield, M.; Dean, A. M.; Fallick, C. J.; Spear, R. J.; Sternhell, S.; Westerman, P. W. *J. Am. Chem. Soc.* 1975, 97, 1482.

(38) Walker, T. E.; London, R. E.; Whaley, T. W.; Barker, R.; Matwiyoff, N. A. *J. Am. Chem. Soc.* 1976, 98, 5807.

(39) King-Morris, M.; Serianni, A. S., manuscript in preparation.

(40) Snyder, J.; Serianni, A. S., unpublished results.

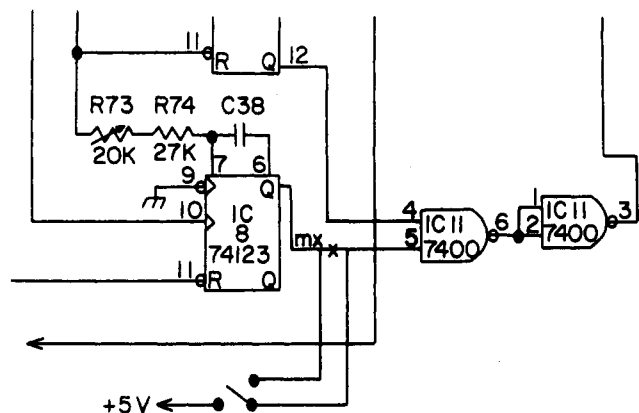


**Figure 10.** Section of the circuit contained on the control PC board in the spectrometer control unit of the Nicolet NT-300 NMR spectrometer. A SPDT toggle switch was connected between IC8 (timer) and IC11 (pulse gate) as shown. The switch was mounted on the rear of the control Unit to prevent inadvertent use of this feature.

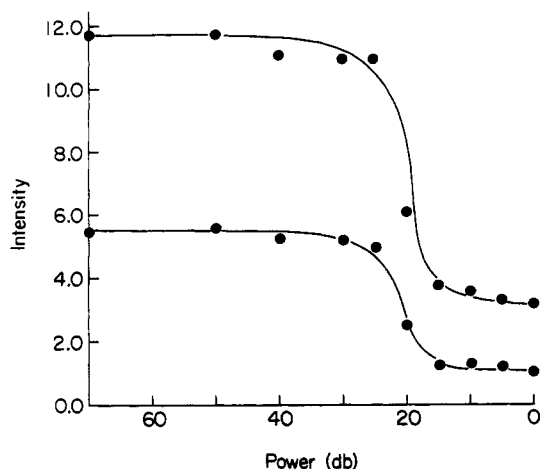
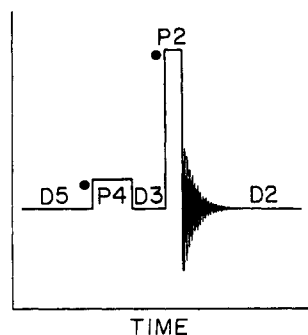


**Figure 11.** The effect of rf power on the signal intensities of C1 of D-[1-<sup>13</sup>C]erythrose after infinite saturation times (15 s). Top curve,  $\beta$ -furanose; bottom curve,  $\alpha$ -furanose. As saturation power is increased (lower db attenuation), equilibrium intensities decrease; after 15 dB attenuation, further power increases have no effect on intensities. To avoid possible secondary effects in the ST spectra, an attenuation value of 12–15 db is used in the experiment. Sample conditions: 0.3 M D-[1-<sup>13</sup>C]erythrose, 50 mM sodium acetate buffer, pH 5.0, 50 °C, 15% (v/v) <sup>2</sup>H<sub>2</sub>O in sample.

**Scheme II**



and analyzed; resonances of the four cyclic forms have been assigned. (c) Linear forms of D-idose (aldehyde, hydrate) have been detected and quantified by <sup>13</sup>C NMR. (d) Preferred solution conformations of the idopyranoses have been examined; evidence for skew forms of  $\alpha$ -D-idopyranose was obtained. (e) Rate constants for ring-opening and -closing of idofuranoses and idopyranoses were measured and compared.

**Acknowledgment.** We recognize the generous assistance from Dr. Mishra at Carnegie-Mellon University in obtaining the 600-MHz <sup>1</sup>H NMR spectra. This work was supported by the Research Corporation and the National Institutes of Health (GM 33791). We also thank Rosemary Patti for typing the manuscript.

### Appendix

**<sup>13</sup>C NMR Saturation-Transfer (ST) on the Nicolet NT-300 Spectrometer: Description of Hardware Modifications and Pulse Program.** The <sup>13</sup>C ST NMR method is a valuable experimental tool for many NMR studies, even when applied in a qualitative fashion to identify nuclei undergoing chemical exchange. The limited use of this experiment may lie in a general perception that it is difficult to implement a protocol to perform this experiment under computer control. We wish to dispel this notion by describing the modifications that can be made on a Nicolet NT-300 FT-NMR, equipped with a 293B pulse programmer, to enable it to conduct the <sup>13</sup>C ST experiment. The manipulation of ST NMR spectra to obtain rate constants can be found in ref 6 and 7 of this paper.

**Hardware Modifications.** Two hardware modifications are necessary. The first of these involves the removal of a factory-installed time limit placed on the length of transmitter pulses (this feature is installed to prevent long (>4.5 ms) high-power FT pulses from damaging probe circuitry). This constraint can be removed by modifying the circuit shown in Figure 10. Once this limit can be removed by the user, caution must be exercised to insure that the spectrometer is operated with the limit in place for routine use to prevent potential damage by unsuspecting operators.

The second modification involves the replacement of two relays in the Broadband Power Amplifier unit (relays K1 and K2), used to switch between high- and low-transmitter power, with faster (<2–3 ms switching times) units; these were purchased from Daico Industries Inc., Compton, CA 90224 (Part no. 100C0076, switchable rf relay SP2T).

**Pulse Program.** The pulse sequence for the <sup>13</sup>C ST experiment is shown in Scheme II. The sequence starts with a relaxation delay (D5) to insure that the system is fully relaxed between pulses. After D5, the low-power transmitter pulse is turned on at the frequency desired for saturation (the on-resonance offset). The saturation interval is determined by P4. After P4, a short (200  $\mu$ s) delay is introduced to trigger a transmitter offset change (for acquisition) and switching to high-power FT for observation. The 90° pulse (P2) is then applied and the data collected over the time D2. The cycle is repeated until sufficient S/N is obtained.

The pulse program used to implement this sequence, written in Nicolet programming language, is as follows:

```

experiment name: SELSAT
experiment title: Selective Carbon Saturation
#1: D4
#2: D3,B
#3: P2/0
#4: A
#5: D2
#6: D5
#7: P4/0 Jump To #1

```

Transmitter frequency alternation (FA) must be activated and the appropriate offset entered to alter SF for data acquisition. The SF value entered in the normal parameters list defines the frequency of saturation. Also, before the experiment is started, low-power transmitter power (TL) must be selected. A list of P4 values (for varying the



saturation time) can also be created by the user.

Transmitter power applied in the low-power mode is controlled by the transmitter attenuator on the spectrometer. The pulse power necessary to achieve saturation must be established empirically by systematically changing the dB attenuation and observing the effect on exchange spectra. A titration-like curve is obtained (Figure 11) which is used to determine the best attenuation for the experiment. Our experiments were conducted at 15 dB attenuation.

The experiment is initiated by the GS command. After entering the number of spectra to be collected (equal to the number of P4 values entered), a file name is chosen under which spectra will be collected and distinguished

from each other by an arithmetically increasing numerical extension. It is also best to include several discarded scans (DG = 2) in the experiment to insure proper pulse sequencing.

It is important to achieve good digital resolution (computer points/hz) in ST spectra if intensities are to be used to evaluate rate constants. Spectra can be collected with fewer points to save disk space and zero-filled during data processing.

**Registry No.** D-Idose, 5978-95-0;  $\alpha$ -D-idofuranose, 41847-67-0;  $\beta$ -D-idofuranose, 40461-75-4;  $\alpha$ -D-idopyranose, 7282-82-8;  $\beta$ -D-idopyranose, 7283-02-5; 5-O-methyl- $\alpha$ -D-xylofuranose, 94707-49-0; 5-O-methyl- $\beta$ -D-xylofuranose, 94707-50-3; D-[1- $^{13}$ C]idose, 70849-26-2; D-glycero-D-[1- $^{13}$ C]idoheptose, 102368-20-7.

## Methyl 2,3-Dideoxy-3-nitro-D-erythro-pentofuranoside, Isomers and Derivatives

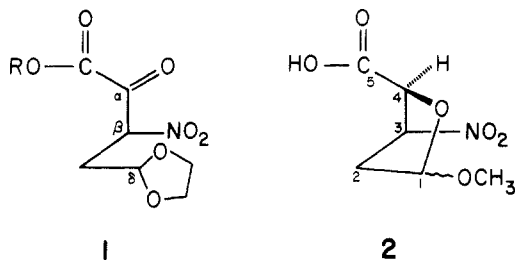
J. F. Weber, J. W. Talhouk, R. J. Nachman, Tian-Pa You, R. C. Halaska, T. M. Williams, and H. S. Mosher\*

Department of Chemistry, Stanford University, Stanford, California 94305

Received December 6, 1985

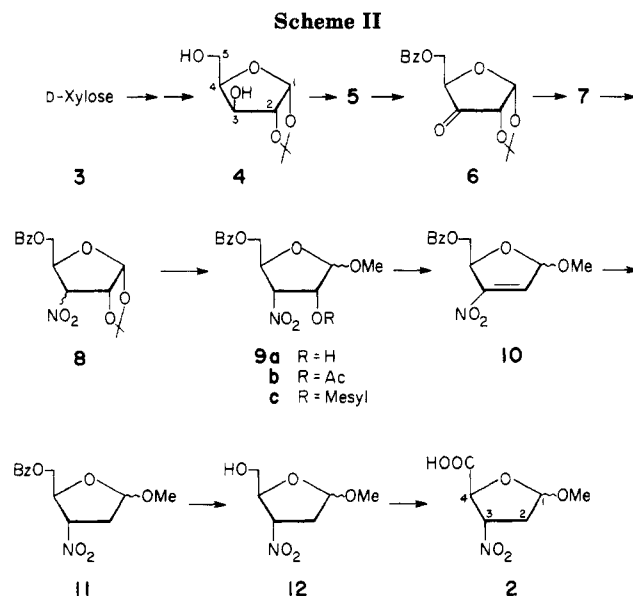
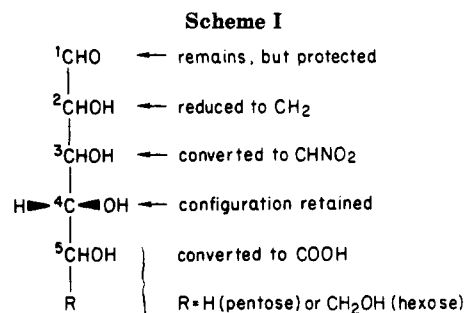
Practical syntheses are described for the versatile intermediates, methyl 2,3-dideoxy-3-nitro-D-erythro-pentofuranoside (12), the corresponding uronic acid (2), and some derivatives, starting from either D-glucose or D-xylose.

In previous studies<sup>1,2</sup> we had prepared the protected  $\delta$ -aldehyde- $\alpha$ -keto- $\beta$ -nitro ester 1 but found it to be too unstable for our projected synthetic purposes.<sup>3,4</sup> We have therefore selected structure 2 as a target molecule, which has the same carbon skeleton and basic functionality with the exception that the  $\alpha$ -keto in 1 is present in reduced



form as the ring oxygen in the furanose derivative 2. The crucial stereochemistry from the standpoint of our projected synthesis is the configuration at C-4 as shown<sup>5</sup> in 2, since all other chiral centers are to be eliminated or modified in subsequent reactions. Thus, any pentose or hexose with the D configuration at C-4 which can undergo the indicated transformations shown in Scheme I could serve as a suitable starting point. Scheme II shows the strategy followed starting with D-xylose and Scheme III with D-glucose.

D-Xylose was an attractive starting material because intermediate 8 was already described.<sup>6</sup> By variations of



the methods reported,<sup>6-15</sup> as shown in Scheme II (4 → 5 → 6 → 7 → 8), the synthesis of 8 has been developed in

(1) Williams, T. M.; Crumbie, R. L.; Mosher, H. S. *J. Org. Chem.* **1985**, *50*, 91.

(2) Crumbie, R. L.; Nimitz, J. S.; Mosher, H. S. *J. Org. Chem.* **1982**, *47*, 4040.

(3) Nachman, R. J. Ph.D. Thesis, Stanford University, 1981.

(4) Williams, T. M.; Mosher, H. S. *Tetrahedron Lett.* **1985**, *26*, 6269.

(5) The numbering system in 2 is chosen to correspond to the precursor carbohydrates.